



Fabrication and electrical transport characterization of high quality underdoped $\text{YBa}_2\text{Cu}_3\text{O}_{7-\delta}$ nanowires

Downloaded from: <https://research.chalmers.se>, 2025-12-05 01:51 UTC

Citation for the original published paper (version of record):

Andersson, E., Arpaia, R., Trbaldo, E. et al (2020). Fabrication and electrical transport characterization of high quality underdoped $\text{YBa}_2\text{Cu}_3\text{O}_{7-\delta}$ nanowires. Superconductor Science and Technology, 33(6).
<http://dx.doi.org/10.1088/1361-6668/ab807e>

N.B. When citing this work, cite the original published paper.

PAPER • OPEN ACCESS

Fabrication and electrical transport characterization of high quality underdoped $\text{YBa}_2\text{Cu}_3\text{O}_{7-\delta}$ nanowires

To cite this article: Eric Andersson *et al* 2020 *Supercond. Sci. Technol.* **33** 064002

View the [article online](#) for updates and enhancements.






IOP | ebooks™

Bringing together innovative digital publishing with leading authors from the global scientific community.

Start exploring the collection—download the first chapter of every title for free.

Fabrication and electrical transport characterization of high quality underdoped $\text{YBa}_2\text{Cu}_3\text{O}_{7-\delta}$ nanowires

Eric Andersson¹, Riccardo Arpaia^{1,2} , Edoardo Trabaldo¹, Thilo Bauch¹ 
and Floriana Lombardi¹ 

¹ Quantum Device Physics Laboratory, Department of Microtechnology and Nanoscience, Chalmers University of Technology, Göteborg SE-41296, Sweden

² Dipartimento di Fisica, Politecnico di Milano, Milano I-20133, Italy

E-mail: floriana.lombardi@chalmers.se

Received 18 October 2019, revised 20 February 2020

Accepted for publication 17 March 2020

Published 23 April 2020



Abstract

We present the fabrication and electrical transport characterization of underdoped $\text{YBa}_2\text{Cu}_3\text{O}_{7-\delta}$ nanowires. The nanowires have been realized without any protective capping layer and they show transport properties similar to those of the parent thin film, demonstrating that they have not been damaged by the nanopatterning. The current-voltage characteristics of the underdoped nanowires show large hysteretic voltage switching at the critical current, in contrast to the flux-flow like characteristics of optimally doped nanostructures, indicating the formation of a self-stabilizing hot spot. These results open up new possibilities for using the underdoped nanowires as single photon detectors and for exploring the underdoped side of the $\text{YBa}_2\text{Cu}_3\text{O}_{7-\delta}$ phase diagram at the nanoscale.

Keywords: high temperature superconductors, underdoped nanostructures, superconducting detectors

(Some figures may appear in colour only in the online journal)

1. Introduction

Investigation of superconducting $\text{YBa}_2\text{Cu}_3\text{O}_{7-\delta}$ (YBCO) nanowires at different levels of oxygen doping can give access to a variety of new experiments to elucidate the still unknown mechanism for high critical temperature superconductors (HTS). It is by now well established that the complex phase diagram of HTS is dominated by various local electronic orders that are intertwined with superconductivity and become stronger in the underdoped region of the phase diagram [1]. All recent activities on HTS nanowires are focused on optimal doping [2–10]. The realization of underdoped nanowires with dimensions comparable to the relevant length scales of the

local electronic orders could help clarify how these orders are related to the high critical temperature phenomenon.

At the same time, underdoped HTS nanowires can be important for the development of quantum limited sensors where a high value of resistivity would increase the sensitivity of the devices. It is well established that the resistivity of HTS thin films increases when going to the underdoped side of the phase diagram [11, 12]. In our previous works we have demonstrated that an increased resistivity helps to improve the flux noise properties of nanowire based superconducting quantum interference devices (nanoSQUIDs) [13–15]. High resistivity is also important for superconducting nanowire based single photon detectors (SNSPDs) where it greatly enhances the sensitivity [16].

However, YBCO has some drawbacks when one is dealing with the fabrication of nanostructures. The material is chemically unstable compared to low critical temperature superconductors (LTS), which makes it difficult to fabricate nanostructures without severe degradation [17–19].



Original content from this work may be used under the terms of the [Creative Commons Attribution 4.0 licence](https://creativecommons.org/licenses/by/4.0/). Any further distribution of this work must maintain attribution to the author(s) and the title of the work, journal citation and DOI.

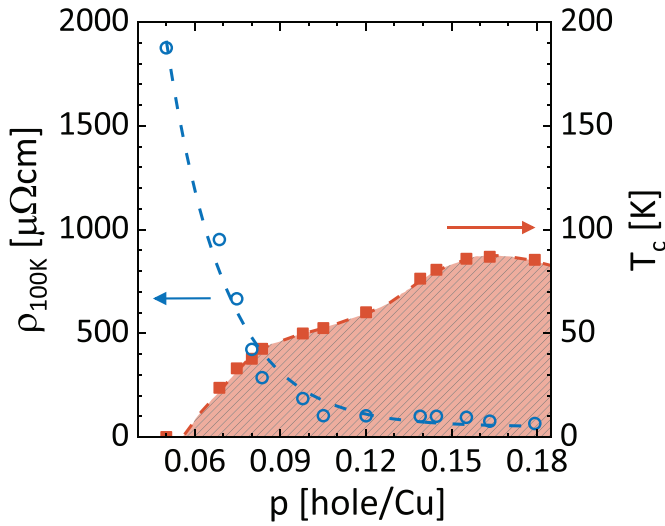


Figure 1. Resistivity at $T = 100$ K (blue open circles) and critical temperature T_c (red filled squares) versus hole-doping level for $t = 30$ nm YBCO thin films. The blue dashed line is an exponential fit to the resistivity data. The data is adapted from [11].

Furthermore, reduction of the hole-doping makes underdoped nanowires much less stable against oxygen out-diffusion which complicates the fabrication process. There are currently only a few reports on the realization of underdoped HTS nanostructures and the results are not very encouraging. The transport properties are severely degraded in comparison to the pristine thin films [20, 21].

In this paper, we present fabrication and electrical transport characterization of 50 nm thick underdoped YBCO nanowires without any protective capping. We demonstrate that the nanowires show properties similar to those of the pristine underdoped thin film which implies that we do not damage the material during the fabrication process. We also discuss the main physical requirements for the nanowires to be employed as SNSPDs. We demonstrate that our underdoped nanowires show large hysteretic voltage switching which indicates self-sustained hot spot formation despite the comparably large thickness. These results pave the way for possible future applications of YBCO nanowires as SNSPDs.

2. Nanowire based single-photon detectors: main requirements

In the original proposal for a SNSPD, by Golt'sman *et al* [22], the absorption of a photon with energy $\hbar\omega \gg 2\Delta$ (where ω and Δ are the frequency of the impinging photon and the gap of the superconductor respectively) creates, through electron-electron and electron-phonon interactions, a local non-equilibrium perturbation with a large number of excited hot electrons. This corresponds to an increased local temperature in the nanowire, above the superconducting transition. The time for this initial thermalization phase τ_{th} must be extremely fast, in general much faster than the electron diffusion time τ_D , to result in the formation of a resistive normal region hot spot which spreads through the width of the nanowire [23]. If

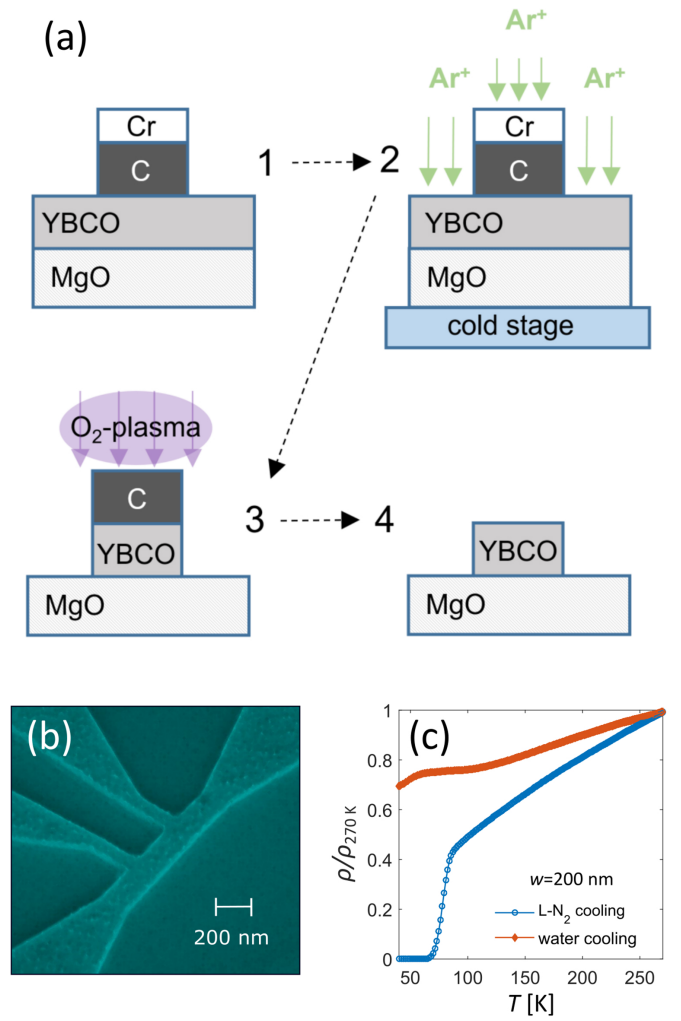


Figure 2. (a) Illustration of the nanowire fabrication process. In step 1, a hard C mask has been deposited and patterned on the YBCO thin film by O_2 plasma etching through an electron-beam lithography defined Cr mask. In step 2, the YBCO not covered by C and the Cr mask is removed with Ar^+ ion milling. In 3, the remaining C on top of the YBCO is etched with a low power O_2 plasma. The final result is shown in 4. (b) False-colour SEM image of a 200 nm wide nanowire with current and voltage leads. (c) Resistivity vs temperature measurement of underdoped nanowires etched with water cooling (red filled diamonds) and liquid nitrogen ($L-N_2$) cooling (blue open circles) of the cold stage during the ion milling in step 2 (panel (a)). Note that only the nanowire etched with $L-N_2$ shows a superconducting transition.

this condition is not realized and the thermalization time τ_{th} of the electrons is larger than their diffusion time $\tau_{D,w} \cong w^2/4D$ (where w is the nanowire width and D the thermal diffusion constant) across the nanowire, the energy of the photon will be smeared over a large area which leads to a weak influence on the superconducting properties and complicates the photon detection [23]. Thus, the formation of the hot spot strongly depends on the electronic properties of the superconducting material and the dimensions of the nanowire. When searching for new materials that can be used for SNSPDs one should therefore focus on systems with low thermal conductivity, once other conditions are satisfied, e.g. a small value of the coherence length [23].

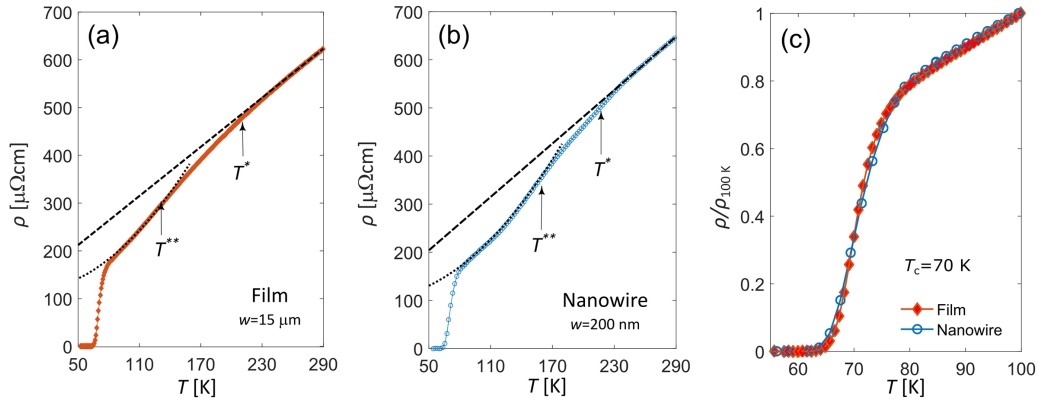


Figure 3. Resistivity versus temperature data for (a) a 15 μm wide strip representing the underdoped film properties ($T_c = 70$ K), (b) a 200 nm wide nanowire and (c) comparison of the microwire and nanowire resistivity normalized at $T = 100$ K. Panel (c) clearly shows that the nanopatterning process does not significantly affect the superconducting transition. The characteristic temperatures T^* and T^{**} are highlighted for comparison in (a) and (b). T^* is the temperature where the resistivity deviates from high temperature linear behaviour and T^{**} the onset of quadratic resistivity behaviour.

At present, the materials that best satisfy these requirements and are commonly used for SNSPDs are granular LTS such as NbN, NbTiN and WSi [16]. An alternative route would be to use HTS [24, 25], in particular YBCO nanowires [2, 26–30], which could help realizing detectors that operate at higher temperatures. It is however challenging to use YBCO for SNSPDs. Apart from the chemical instability of the material during the fabrication process, the main issue comes from the high thermal conductivity of optimally doped YBCO ($\kappa \approx 15 \text{ W m}^{-1} \text{ K}^{-1}$ in the normal state [31]) which would prevent the stabilization of a hot spot.

Because of the high thermal conductivity, observation of highly hysteretic current-voltage characteristics (IVCs) in optimally doped YBCO nanowires (indicative of the formation of a self-stabilizing hot spot [32]) is hard to achieve. A possible route towards YBCO based SNSPDs is therefore to reduce the thermal conductivity by increasing the resistivity of the samples. According to the Wiedemann-Franz law, which has recently been demonstrated to hold for cuprate superconductors [33], the thermal conductivity $\kappa = LT/\rho$ (where $L = \pi^2 k_B^2 / 3e^2$ is the Lorenz number) can be reduced by increasing the resistivity ρ . This approach is utilized in LTS where ρ is increased by introducing granularity in the thin films [34], which brings the system closer to the metal insulator transition. In YBCO, a different strategy has to be adapted since grain boundary formation significantly reduces the critical current density J_c of the films [35].

It has been shown that hysteretic IVCs can be achieved in YBCO by maximizing the Joule heating, i.e. maximizing the critical current I_c and the normal state resistance R_N , since Joule heating in the normal state helps to stabilize the hot spot [36]. Hysteretic IVCs have been observed in high quality (high J_c) YBCO nanowires that are only a few unit cells thick (high R_N) [5, 30]. However, because of the small thickness, these nanowires have problems with stability over time and it is very challenging to fabricate long, meandering structures that are required for SNSPDs. An alternative approach to increase ρ in YBCO is to reduce the hole-doping level p , since the resistivity

increases exponentially with decreasing oxygen doping level, see figure 1. By using underdoped YBCO it might be possible to achieve self-stabilizing hot spot formation in thicker and larger nanowires that are more stable compared to the ultrathin optimally doped ones.

3. Fabrication of underdoped nanowires

50 nm thick YBCO thin films were deposited by pulsed laser deposition on MgO(110) substrates at 760 $^\circ\text{C}$, 0.8 mbar oxygen pressure and with a laser fluency of 2 J cm^{-2} . To achieve the desired level of oxygen doping, the films were slowly cooled down in a low steady flow of oxygen resulting in a background pressure $P \sim 10^{-4}$ – 10^{-5} mbar (see [11] for a detailed description of the deposition process).

For the nanopatterning we use an improved process, previously developed for slightly overdoped YBCO nanowires, where the YBCO is etched with gentle Ar^+ -ion milling through an electron-beam lithography defined amorphous carbon mask. The schematic flow of the process is shown in figure 2(a) (see [37–39] for a more detailed description). The patterned nanowires are 450 nm long and 100–600 nm wide.

To reduce the overheating and to preserve the properties of the nanowires during the Ar^+ -ion etching, the sample stage was cooled with liquid nitrogen instead of standard water cooling. Resistivity measurements of the nanowires show that with water cooling the 200 nm wide nanowires are not superconducting, while with liquid nitrogen cooling there is a sharp transition around 75 K, see figure 2(c). Another important difference in the fabrication process, compared to our earlier works, is that the removal of the amorphous carbon mask left on the YBCO after the Ar^+ -ion milling is done with an extremely gentle oxygen reactive ion etching process. A very low power (15 W) microwave oxygen plasma is used to remove the carbon mask. For higher powers the superconducting transition of the nanowires is broadened indicating damage to the material.

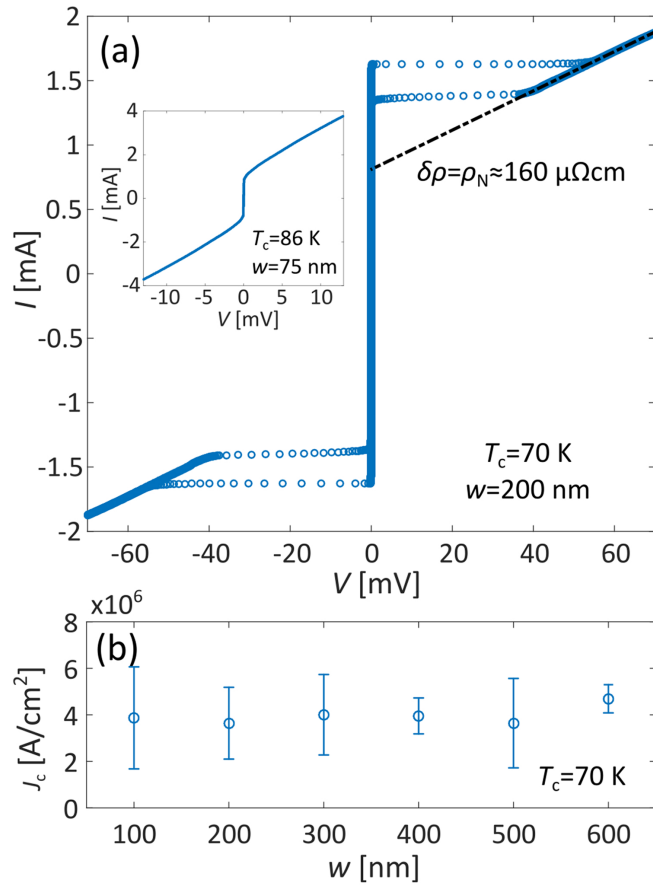


Figure 4. (a) typical IVC of a 50 nm thick underdoped nanowire at $T = 4.5$ K and (b) width dependence of the critical current density J_c . Each point represent data from four nanowires patterned on the same thin film. The inset in (a) shows a typical IVC of a slightly overdoped nanowire.

4. Electrical transport characterization

In figure 3, the resistivity vs temperature $\rho(T)$ of a nanowire and a wide strip (from here on referenced to as ‘film’), are presented and compared. A first indication that the nanowires are pristine after the patterning process is that the value of the resistivity at room temperature is not significantly increased compared to the film (645 $\mu\Omega\text{cm}$ compared to 623 $\mu\Omega\text{cm}$, see panel (b) and (a) of figure 3). In case of induced defects or changes in the doping due to oxygen out-diffusion caused by the etching, the difference in ρ would have been significant. Moreover, from the comparison of the superconducting transition of the nanowire and the film, see figure 3(c), it is evident that the superconducting transition temperature T_c is unchanged and there is very little additional broadening of the superconducting transition induced by the nanowire.

Since our underdoped nanowires are without any protective gold capping layer, one can also study the normal state transport properties of the material. The YBCO (and HTS in general) phase diagram is very rich in the underdoped side with various local orders simultaneously at play [1]. Signatures of variation of the Fermi surface topology and

transport mechanisms are also visible in the electronic transport. An interesting question is if these orders are present in nanowires of reduced dimensions. In figure 3, the characteristic temperatures T^* and T^{**} are pointed out. The pseudogap temperature T^* signifies the crossover from the strange metal phase ($\rho \propto T$) [40] to the pseudogap phase in HTS (connected to the breaking of the Fermi surface and the formation of Fermi arcs [41] at T^*) in the underdoped regime. The temperature T^{**} , which is lower than T^* , instead indicates a crossover to more Fermi-liquid like ($\rho \propto T^2$) transport behaviour. T^* and T^{**} does not change significantly when reducing the dimensions (see figures 3(a) and (b)). Hence the physical properties of the film and the nanowire are the same.

Figure 4(a) shows the IVC for a typical underdoped nanowire ($p \approx 0.13$ or $7-\delta \approx 6.75$ [42]) measured at $T = 4.5$ K. It shows large hysteretic voltage switching at the critical current I_c , indicative of a self-sustained hot spot [32]. For comparison, a typical IVC of a slightly overdoped YBCO nanowire with the same thickness is shown in the inset of figure 4(a). For overdoped nanowires, the IVC is flux-flow like, without any sign of voltage switching, in spite of the narrower width ($w = 75$ nm). The difference has to be attributed to the higher resistivity in the underdoped case, leading to a reduced thermal conductivity which promotes Joule heating and the self-stabilization of the hot spot. Another fact that supports this hypothesis is that only the nanowires with the highest J_c (where Joule heating is maximized) show voltage switching, while the nanowires with low J_c show flux-flow behaviour. In the overdoped regime it is still possible to observe hysteretic voltage switching if the thickness is reduced to $t = 10$ nm and the width $w < 100$ nm [30]. However, such extreme dimensions result in instability of the electrical properties over long periods of time.

The dynamical resistivity, $\delta\rho = dI/dV \times A/l$ where A is the cross-sectional area of the nanowire and l the length, is extracted from the slope of the IVC in the normal state (see figure 4(a)). The value $\delta\rho = 160 \mu\Omega\text{cm}$ (corresponding to $R \approx 76 \Omega$) is close to the normal resistivity ρ_N of the nanowire just above the superconducting transition (see figure 3(b)). This indicates that the whole nanowire volume turns resistive after the switch, proving effective spreading of the self-stabilizing hot spot.

Since a high value of I_c is important for the voltage switching to occur in the nanowires [30], we have measured the critical current density J_c dependence as a function of the width (see figure 4(b)). J_c is approximately independent of the width down to $w = 100$ nm which enables the realization of even narrower structures in the future. The value of the critical current density $J_c \approx 4 \times 10^6 \text{ A cm}^{-2}$ is only half of the best values measured in underdoped YBCO nanowires capped with Au [11], which indicates that the Au capping is indispensable for achieving the highest J_c .

5. Conclusions

We have presented the realization of high-quality underdoped YBCO nanowires. They are without metallic capping in order

to study the normal state of HTS on the nanoscale. The doping level of the nanostructures is the same as that of the parent thin film and the transport properties are unaffected by the fabrication process. Despite the relatively large thickness ($t = 50$ nm), the IVCs show large hysteretic voltage switching that in optimally doped/overdoped YBCO nanowires is achieved only at extreme thicknesses (<10 nm) and widths (<100 nm). This demonstrates that for underdoped nanowires the increase in resistivity relates to a reduction of the thermal conductivity, in agreement with the Wiedemann-Franz law. The large hysteretic voltage switching makes underdoped nanowires attractive for application as SNSPDs. There are, however, some substantial problems to address. The normal state resistance of the nanowires after the switch is not very large ($R \approx 76 \Omega$) which would limit the sensitivity in a SNSPD setup and cause problems with latching. Furthermore, the nanowires presented here are probably too thick for single photon sensitivity. To address these problems, one possibility is to reduce the thickness to values which are more common for SNSPDs ($t \approx 5$ – 10 nm) and increase (decrease) the nanowire length (width) to get higher resistance. This, however, represents a challenge since thinner and longer wires would be more unstable over time and suffer from a significant reduction of J_c [28]. Another way to increase the resistance is to further reduce the doping. Here we have presented devices with $T_c = 70$ K. In principle there should be no major issues in making nanowires with T_c in the range of 50 K which would show higher resistivity, lower thermal conductivity and therefore larger hysteresis, all crucial properties for SNSPDs

Acknowledgments

This work was supported in part by the Knut and Alice Wallenberg Foundation (KAW) and in part by the Swedish Research Council (VR). R A is supported by VR under the project 2017-00382. Myfab is acknowledged for support and for access to the nanofabrication laboratories at Chalmers.

ORCID iDs

Riccardo Arpaia  <https://orcid.org/0000-0003-4687-2376>
 Thilo Bauch  <https://orcid.org/0000-0002-8918-4293>
 Floriana Lombardi  <https://orcid.org/0000-0002-3478-3766>

References

- [1] Keimer B, Kivelson S A, Norman M R, Uchida S and Zaanen J 2015 *Nature* **518** 7538
- [2] Amari P et al 2018 *Supercond. Sci. Technol.* **31** 015019
- [3] Lam S, Bendavid A and Du J 2019 *Nanotechnology* **30** 325301
- [4] Rouco V et al 2019 *Nano Lett.* **19** 4174
- [5] Lyatti M, Wolff M A, Savenko A, Kruth M, Ferarri S, Poppe U, Pernice W, Dunin-Borkowski R E and Schuck C 2018 *Phys. Rev. B* **98** 054505
- [6] Ostrove C and Reichl L E 2019 *Phys. B* **561** 79
- [7] Cho E Y, Zhou Y W, Cho J Y and Cybart S A 2018 *Appl. Phys. Lett.* **113** 022604
- [8] Trbaldo E, Arpaia R, Baghdadi R, Andersson E, Lombardi F and Bauch T 2017 *IEEE Trans. Appl. Supercond.* **27** 2660306
- [9] Baghdadi R, Arpaia R, Charpentier S, Golubev D, Bauch T and Lombardi F 2015 *Phys. Rev. Appl.* **4** 014022
- [10] Baghdadi R, Arpaia R, Bauch T and Lombardi F 2014 *IEEE Trans. Appl. Supercond.* **25** 1100104
- [11] Arpaia R, Andersson E, Trbaldo E, Bauch T and Lombardi F 2018 *Phys. Rev. Mater.* **2** 024804
- [12] Ohkubo M 1990 *Solid State Commun.* **74** 785
- [13] Arpaia R, Arzeo M, Baghdadi R, Trbaldo E, Lombardi F and Bauch T 2017 *Supercond. Sci. Technol.* **30** 014008
- [14] Trbaldo E, Pfeiffer C, Andersson E, Arpaia R, Kalaboukhov A, Winkler D, Lombardi F and Bauch T 2019 *Nano Lett.* **19** 1902
- [15] Trbaldo E, Arpaia R, Arzeo M, Andersson E, Golubev D, Lombardi F and Bauch T 2019 *Supercond. Sci. Technol.* **32** 073001
- [16] Natarajan C M, Tanner M G and Hadfield R H 2012 *Supercond. Sci. Technol.* **25** 063001
- [17] Larsson P, Nilsson B and Ivanov Z G 2000 *J. Vac. Sci. Technol. B* **18** 25
- [18] Xu K and Heath J R 2008 *Nano Lett.* **8** 3845
- [19] Papari G, Carillo F, Stornaiuolo D, Longobardi L, Beltram F and Tafuri F 2012 *Supercond. Sci. Technol.* **25** 035011
- [20] Bonetti J A, Caplan D S, Van Harlingen D J and Weissman M B 2004 *Phys. Rev. Lett.* **93** 087002
- [21] Carillo F, De Luca G M, Montemurro D, Papari G, Salluzzo M, Stornaiuolo D, Tafuri F and Beltram F 2012 *New J. Phys.* **14** 083025
- [22] Gol'tsman G N, Okunev O, Chulkova G, Lipatov A, Semenov A, Smirnov K, Voronov B and Dzardanov A 2001 *Appl. Phys. Lett.* **79** 705
- [23] Vodolazov D Y 2017 *Phys. Rev. Appl.* **7** 034014
- [24] Charpentier S, Arpaia R, Gaudet J, Matte D, Baghdadi R, Löfwander T, Golubev D, Fournier P, Bauch T and Lombardi F 2016 *Phys. Rev. B* **94** 060503
- [25] Romano P, Riccio M, Guarino A, Martucciello N, Grimaldi G, Leo A and Nigro A 2018 *Measurement* **122** 502
- [26] Curtz N, Koller E, Zbinden H, Decroux M, Antognazza L, Fisher Ø and Gisin N 2010 *Supercond. Sci. Technol.* **23** 045015
- [27] Arpaia R, Ejrnaes M, Parlato L, Tafuri F, Cristiano R, Golubev D, Sobolewski R, Bauch T, Lombardi F and Pepe G P 2015 *Phys. C* **509** 16
- [28] Arpaia R, Ejrnaes M, Parlato L, Cristiano R, Arzeo M, Bauch T, Nawaz S, Tafuri F, Pepe G P and Lombardi F 2014 *Supercond. Sci. Technol.* **27** 044027
- [29] Ejrnaes M, Parlato L, Arpaia R, Bauch T, Lombardi F, Cristiano R, Tafuri F and Pepe G P 2017 *Supercond. Sci. Technol.* **30** 12LT02
- [30] Arpaia R, Golubev D, Baghdadi R, Ciancio R, Dražić G, Orgiani P, Montemurro D, Bauch T and Lombardi F 2017 *Phys. Rev. B* **96** 064525
- [31] Sutherland M, Hawthorn D G, Hill R W, Ronning F, Wakimoto S, Zhang H, Proust C, Boaknin E, Lupien C and Taillefer L 2003 *Phys. Rev. B* **67** 174520
- [32] Tinkham M 2004 *Introduction to Superconductivity* (Mineola, New York: Dover Publications)
- [33] Michon B et al 2018 *Phys. Rev. X* **8** 041010
- [34] Yurchenko V V, Ilin K, Meckbach J M, Siegel M, Qviller A J, Galperin Y M and Johansen T H 2013 *Appl. Phys. Lett.* **102** 252601
- [35] Levi D, Shaulov A, Frydman A, Koren G, Shapiro B Y and Yeshurun Y 2013 *EPL* **101** 67005
- [36] Golubev D, Lombardi F and Bauch T 2014 *Phys. C* **506** 174

- [37] Nawaz S, Arpaia R, Lombardi F and Bauch T 2013 *Phys. Rev. Lett.* **110** 167004
- [38] Arpaia R, Nawaz S, Lombardi F and Bauch T 2013 *IEEE Trans. Appl. Supercond.* **23** 1101505
- [39] Nawaz S, Arpaia R, Bauch T and Lombardi F 2013 *Phys. C* **495** 07011
- [40] Barišić N, Chan M K, Li Y, Yu G, Zhao X, Dressel M, Smontara A and Greven M 2013 *Proc. Natl Acad. Sci.* **110** 12235
- [41] Norman M R *et al* 1998 *Nature* **392** 6672
- [42] Ohkubo M, Kachi T and Hioki T 1990 *J. Appl. Phys.* **68** 1782